BULLETIN OF THE EARTHQUAKE
RESEARCH INSTITUTE
UNIVERSITY OF TOKYO
Vol. 65 (1990) pp. 33-48

Upper Crustal Structure under the Central Part of Japan: Miyota-Shikishima Profile

Tsutomu SASATANI[1], Toshikatsu YOSHII[2], Akira IKAMI[3],
Toshikazu TANADA[4]*, Tsukasa NISHIKI[2]**
and Susumu KATO[1]***

1) Faculty of Science, Hokkaido University
2) Earthquake Research Institute, The University of Tokyo
3) School of Science, Nagoya University
4) Faculty of Marine Science and Technology, Tokai University

(Received December 28, 1989)

Abstract

In October 1982, a seismic refraction experiment was conducted by the Research Group for Explosion Seismology in the Miyota-Shikishima Profile in Nagano and Yamanashi Prefectures, central Japan. Five shots were fired on the 60 km-long profile. The upper crustal structure derived from travel-time data is simple and has a high velocity gradient; 4.0 km/s at the surface to 6.0 km/s at about 2.5 km depth. Based on the amplitude-distance pattern of the refraction phases, we confirmed the existence of the velocity gradient. A few explosive sources generated clear S waves with amplitudes large enough to be read. We obtained an average POISSON's ratio of around 0.246 in the uppermost crust from S to P travel time ratios. The other later arrivals were interpreted as reflected phases from a deep interface, the Conrad discontinuity. We modeled the interface shape by the ray-tracing technique. The interface inclines teward the north by about 20°.

* Now at Hot Springs Research Institute, Kanagawa, Japan.
** Now at Japan Petroleum Exploration Co. Ltd., Tokyo, Japan.
*** Now at Century Research Center Co. Ltd., Tokyo, Japan.

1. Introduction

The fourth explosion seismic observation experiment under the Japanese Earthquake Prediction Project was conducted in October, 1982 along a profile from Miyota, Nagano Prefecture, to Shikishima, Yamanashi Prefecture. The profile lies near the central part of the Fossa Magna, which is known as the greatest topographic depression in central Honshu. The total length of the profile is about 60 km (Fig. 1). In the area around the profile, no active faults have been found and seismic activity has been low (RESEARCH GROUP FOR ACTIVE FAULTS, 1980). In this paper, the results of interpretation of these explosion data are presented. The fundamental data such as shot locations and observation sites, travel times, record sections, etc. are presented in a separate paper (RESEARCH GROUP FOR EXPLOSION SEISMOLOGY (RGES), 1986).

Previous studies on the three profiles conducted in 1979, 1980 and 1981 (Fig. 1) under the Japanese Earthquake Prediction Project revealed a

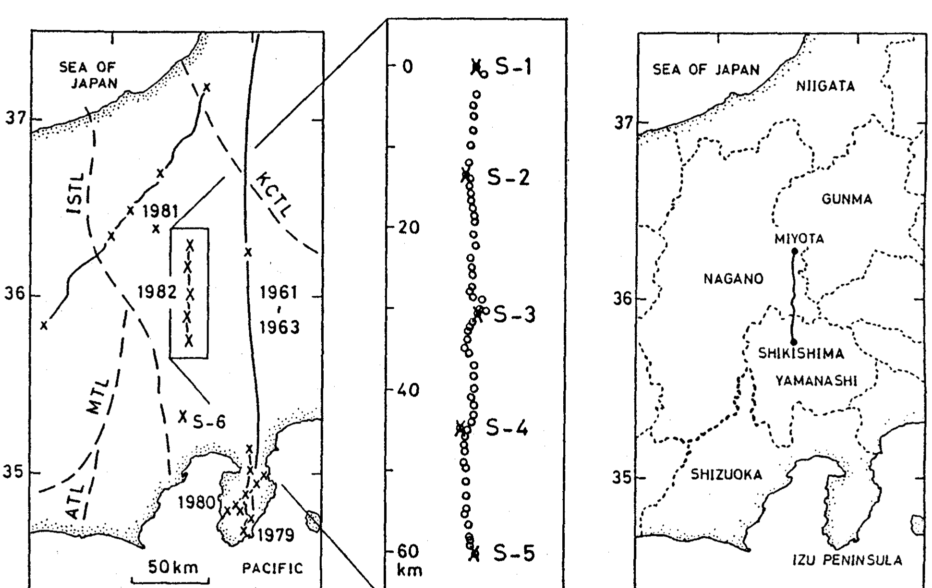

Fig. 1. (a) Tectonic lines in central Japan (broken lines) and the refraction profiles by RGES (solid lines with crosses, which indicate shot points). MTL, Median teconic line; ATL, Akaishi tectonic line; ISTL, Itoigawa-Shizuoka tectonic line; KCTL, Kashiwazaki-Choshi tectonic line. The Fossa Magna lies between ISTL and KCTL. (b) Shot (crosses) and observation points (open circles) of the 1982 experiment. (c) Map showing prefectures and places quoted in this study.

highly heterogeneous upper crust beneath the Izu Peninsula and beneath the profile from south-western Niigata Prefecture to western Nagano Prefecture (ASANO *et al.*, 1982; YOSHII *et al.*, 1985; IKAMI *et al.*, 1986). The present study, however, shows a simple upper crustal structure beneath the Miyota-Shikishima profile.

2. Summary of Explosion Experiments

The total profile length is approximately 60 km and about 60 temporal stations were arranged along it. The average station spacing is about 1 km. Five shots on the profile and a shot about 50 km south of the profile were fired. Dynamite from 300 kg to 800 kg was detonated in bore holes 50 m to 70 m deep. Shot and observation points are shown in Fig. 1 and shot point locations, shot times and charge weights are listed in Table 1. The seismic data were recorded on portable cassette-recording seismographs, each equipped with a 2-Hz vertical component seismometer (L-22D, Mark Products Co. Ltd.). The seismic signal was recorded in FM or PCM formats. The frequency response of the recording system was flat in the range 0.5 Hz to 30 Hz. Every chronometer was checked against JJY, a Japanese standard time signal broadcast by radio, before and after the recording time of the seismic signals. When the time signal could be clearly received during recording time, it was recorded together with a seismic signal on a separate channel. Therefore, time accuracy was kept better than 0.01 s.

In the early experiment along longitudinal line 139°E(1961–1963 in Fig. 1), about 50 km east of the present profile, refraction phases from the Conrad discontinuity were clearly observed (HOTTA *et al.*, 1964). The shot point S-6 about 50 km south of the present profile (Fig. 1) was chosen for the purpose of observing the reflected phases from this discontinuity. However, the record section of shot S-6 (Fig. 3-6 in RGES, 1986) shows no distinct later arrivals. Therefore, observed data from S-6 were not

Table 1. Shot time, location of shot point, and charge size.

Shot	Date	Time	Latitude	Longitude	Height	Charge
S-1	1982 Oct. 29	01 : 22 : 00.72	36°17′29.3″N	138°32′53.5″E	861 m	500 kg
S-2	Oct. 28	01 : 12 : 00.36	36 10 19.8	138 32 0.5	864	400
S-3	Oct. 28	01 : 02 : 00.10	36 1 2.2	138 32 53.4	1140	300
S-4	Oct. 28	01 : 22 : 00.00	35 53 28.1	138 31 30.0	1208	400
S-5	Oct. 29	01 : 02 : 00.17	35 45 13.4	138 32 38.7	730	500
S-6	Oct. 29	01 : 12 : 00.08	35 19 47.2	138 30 7.8	480	800

used in the following analysis.

3. Interpretation

An example of the record section is given in Fig. 2 (for all sections, see RGES, 1986). Impulsive first arrivals were obtained on the majority of the records. In addition to the first arrivals, we can see later arrivals (denoted by "S" and "R") correlated from trace to trace. We can more clearly see these arrivals on the other record sections as shown in Fig. 10. An interpretation of the later arrivals is described a later section.

To obtain the velocity near the ground surface, observations with about 100 m station spacing were carried out at six points near each shot point. These travel time plots gave the same velocity of about 4.0 km/s regardless of the shot point (RGES, 1986). Thus we assumed this velocity for the surface layer along the profile.

3.1 Travel times of the first arrivals

Figure 3 shows the travel time plots of the first arrivals with a reduction velocity of 6.0 km/s. The travel-time curves are smooth, and an apparent velocity around 6.0 km/s can be observed through the profiles. Except for the S-1 plots, intercept times are very small (less than about 0.3 s). On the other hand, the apparent velocity for shots S-2 to S-5 becomes smaller than 6.0 km/s near shot point S-1. These features suggest that the surface layer is thin and that the seismic basement has a velocity of about 6.0 km/s and dips to the north near the shot point S-1.

The time-term method was applied to interpret the travel time data. First we assumed a constant velocity in the refractor and obtained the velocity of 5.97 km/s in it. Figure 4(a) shows the time terms of the basement along the profile. Assuming the constant velocity of the surface layer, we obtained the shape of the basement boundary, which is approximately flat except at both ends (Fig. 4(b)).

A detailed inspection of the travel time plots (Fig. 3) indicates that the apparent velocity slightly increases with distance except near the shot S-1. This may imply a velocity increase with depth in the basement layer. Then we applied the time-term method assuming that the velocity is a linear function of distance (YOSHII and ASANO, 1972). The result is $Vp=5.70+0.00457*D$, where Vp is velocity in km/s at a shot distance D in km. Figure 4(c) shows the time terms obtained based on the above assumption. They are somewhat smaller than those obtained assuming the constant velocity (Fig. 4(a)). The shape of the basement boundary obtained

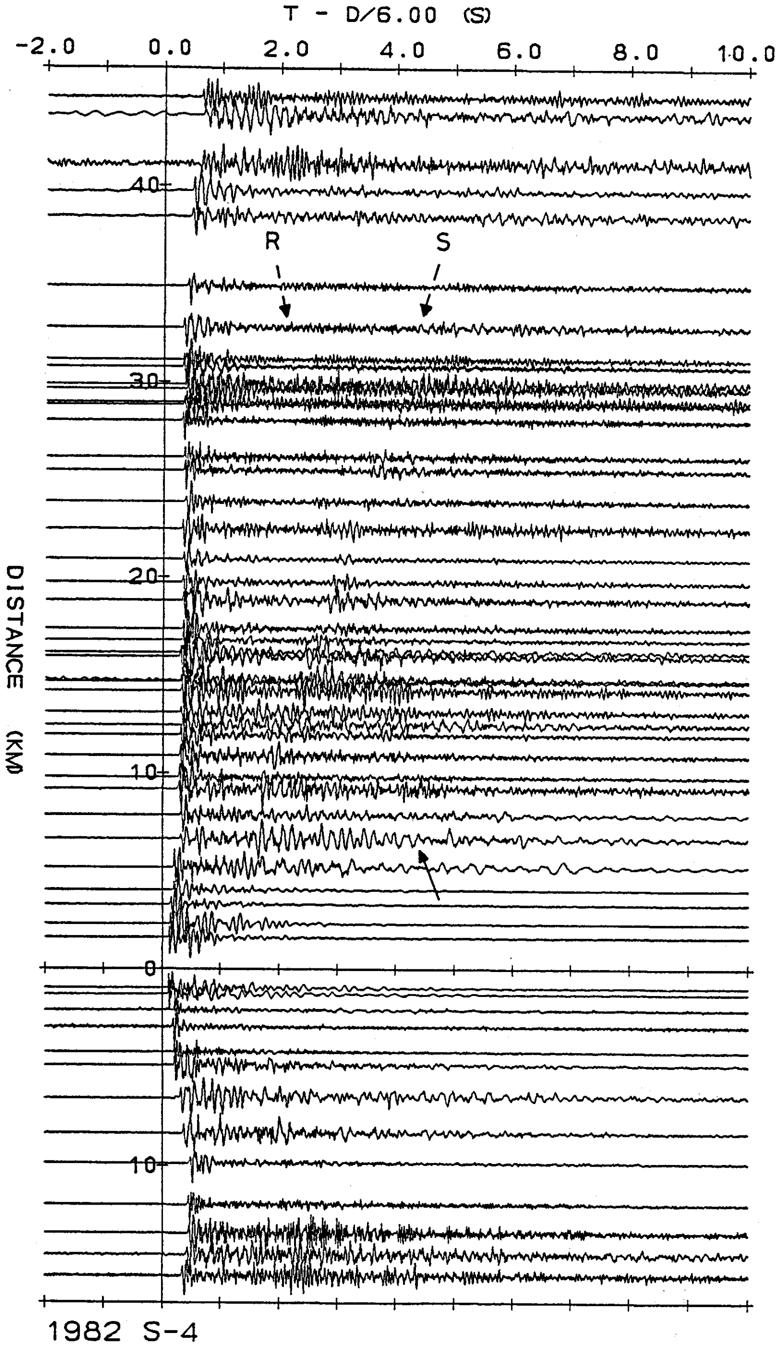

Fig. 2. Record section for S-4. Arrows indicate direction of phases "S" and "R".

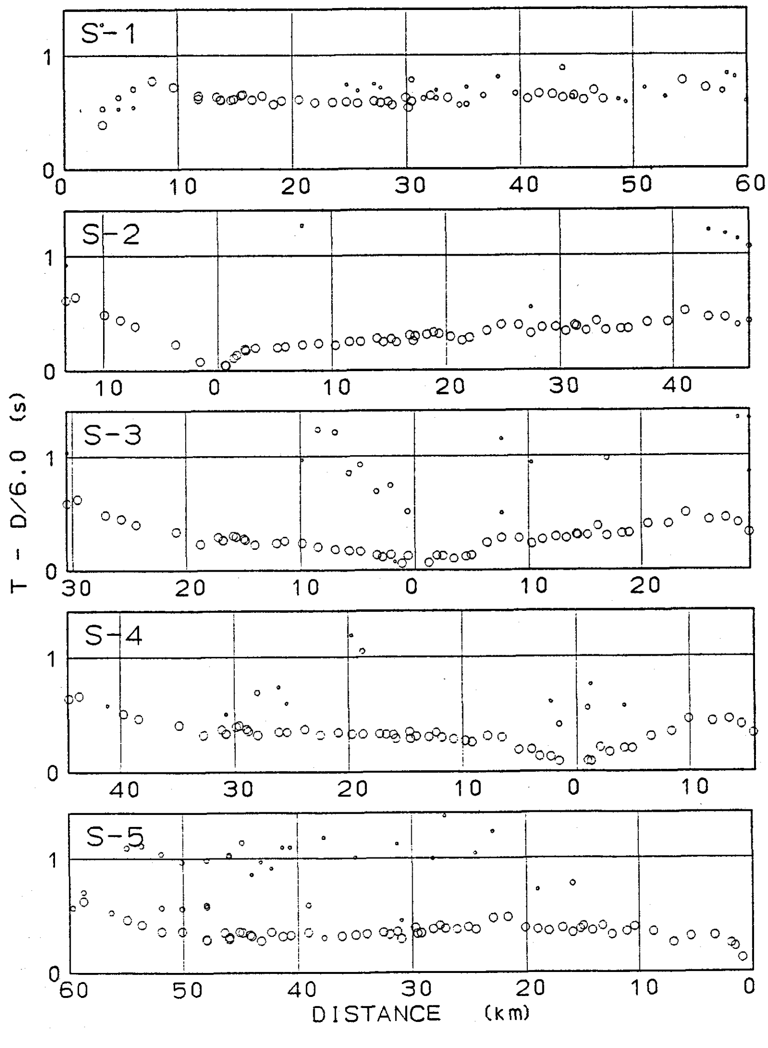

Fig. 3. Reduced travel time plots. Reduction velocity is 6 km/s. Symbols denote grades in reading arrival time: Large, middle and small circles mean "very good", good", and "fairly good", respectively.

from Fig. 4(c) is approximately the same as shown in Fig. 4(b), but the depth of the boundary is shallower by 200–300 m than in Fig. 4(b) in the range of S2–S4. The velocity in the basement layer increases as shown in Fig. 5, which was derived from above formula. For comparison's sake, the velocity-depth profile derived from data around Nagano Prefecture (IKAMI *et al.*, 1986) is also shown by a dashed line. The velocity gradient in the present profile is larger than that obtained beneathe Nagano Prefecture. The crustal structures derived from two time-term methods are

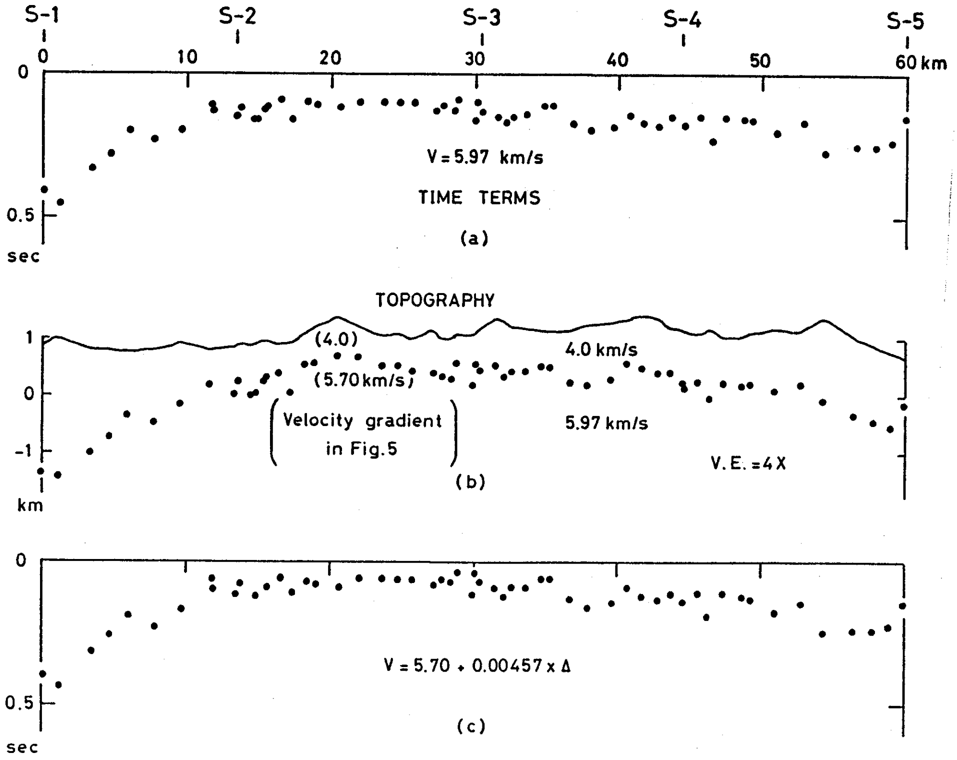

Fig. 4. (a) Time terms obtained by assuming a constant velocity in the refractor. (b) Topography and crustal structures derived from both time terms in (a) and (c). Values with parentheses are those derived from time terms in (c). Note that the model is displayed with vertical exaggeration of 4:1. (c) Time terms obtained by assuming that the velocity is a linear function of distance.

summarized in Fig. 4(b).

3.2 Amplitude study of the first arrivals

BANDA *et al.* (1982) demonstrated, on the basis of synthetic seismograms, that interpretation of the amplitude data led to a more reliable estimate of velocity-depth structure of the upper crust. Then we tried to study the amplitude-distance pattern of the first arrivals to confirm the velocity gradient obtained above (Fig. 5). The maximum amplitudes (peak-to-peak) of the first cycle were read in μm/s. The amplitude-distance data were compared with those obtained from synthetic seismograms for assumed velocity models. We used the reflectivity method to calculate the synthetic seismograms (FUCHS and MÜLLER, 1971; SASATANI, 1985). This technique is valid at all frequencies but requires velocity models consisting of laterally homogeneous and isotropic layers. The time terms

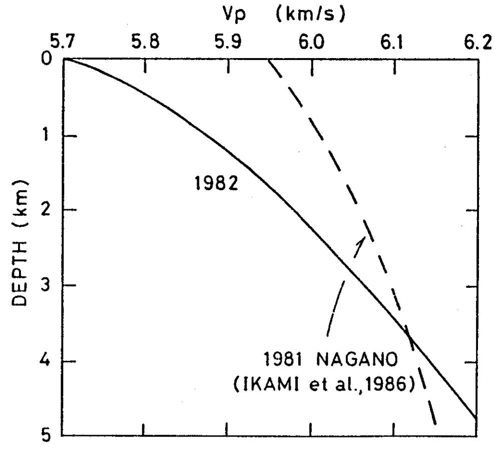

Fig. 5. Velocity-depth relation obtained in the present study (solid line) and that in profile A-4NE around Nagano Prefecture (dashed line; IKAMI *et al.*, 1986). Depths are taken from the top of the basement layer.

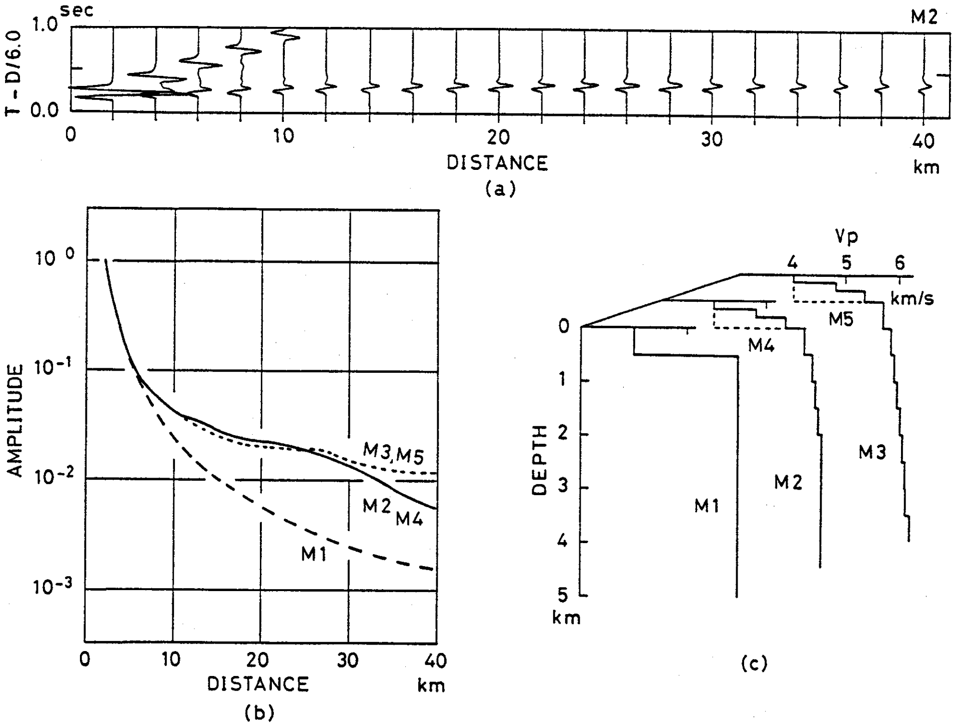

Fig. 6. (a) An example of a synthetic record-section with a dominant frequency of 10 Hz for model M2. The amplitudes are multiplied by the distance. (b) The amplitude-distance curves for five models (M1 to M5). (c) The velocity profiles for these models.

obtained (Fig. 4) may indicate that the basement from the shot point S-2 to the shot point S-4 is approximately flat. Then we did an amplitude study for the data from shots S-2, S-3 and S-4. In the calculation of synthetic seismograms, we ignored the influence of attenuation on the amplitude of the first arrival, because this influence was not so strong in a short distance range (BANDA *et al.*, 1982).

Five velocity-depth models (M1 to M5) were constructed on the basis of interpretation of travel time data. M1 is a single-layered model with a constant velocity (Fig. 6(c)). Models M2 to M5 have velocity gradients; they have the same gradient in a depth range of 1 to 2.5 km, but different surface layers and different thicknesses of the gradient zone (Fig. 6(c)). An example of a synthetic record section (vertical ground velocity with a dominant frequency of 10 Hz) is given for model M2 at the top of Fig. 6, and the amplitudes of each trace are multiplied by the distance for a more accurate reading of the amplitudes. The resulting amplitude-distance curves for five models are displayed in Fig. 6(b). The travel

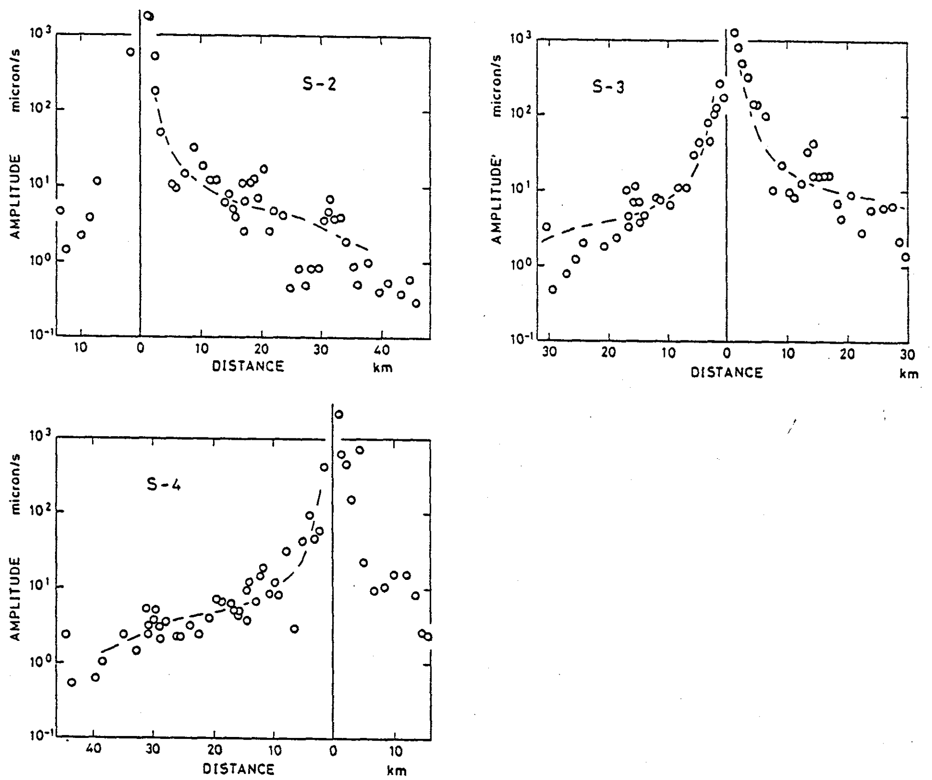

Fig. 7. Amplitude data (open circles) for the first arrivals and amplitude-distance curve (dashed line) calculated from model M2.

time character of these models is approximately the same. The amplitude-distance curve for model M1 is significantly different from the gradient models. The curve for model M2(M3) is essentially indentical to that for model M4(M5). This implies that the surface layers have no influence on the amplitude-distance curve. The thickness of the gradient zone rather influence the amplitude-distance pattern; a decrease in the thickness of the gradient zone leads to a faster drop off of the amplitudes with distance.

Amplitude data for shots S-2, S-3 and S-4 are plotted in Fig. 7. Although the scatter in the data is large, the data show amplitude-distance behavior characterized by a rapid decrease in the first 10 km and a smooth decay out to about 40 km. This behavior may be explained by the amplitude-distance curves for the gradient models (Fig. 6(b)). Since amplitude data exhibit a considerable decrease beyond a distance of 30 km, we prefer model M2 or M4; in Fig. 7, the amplitude-distance curve for model M2 is shown by a dashed curve, which was visually adjusted to the observed data. However, we have no strong reason to deny model M3 or M5 because of the large scatter in the data. Nevertheless, the amplitude study of the first arrivals provided good evidence for a strong velocity gradient in the uppermost crust.

3.3 Travel times of the later arrivals

The later arrivals denoted by "S" in Fig. 2 have an apparent velocity of about 3.5 km/s (Fig. 8). Judging from the apparent velocity rotio of the first to the later arrivals (6.0/3.5=1.71, which is the generally observed value for Vp/Vs in the upper crust), these arrivals can be regarded as S-waves radiated directly from the explosive source. Recently combined analysis of P and S wave data from seismic refraction profiles has led to the derivation of a POISSON's ratio model for the crust (*e.g.*, ASSUMPÇAO and BAMFORD, 1978; EL-ISA *et al.*, 1987; HOLBROOK *et al.*, 1988). POISSON's ratio is an important constraint on estimates of the composition and physical state of the crust. Unfortunately, in this experiment not all of the shots generated good S waves and not all stations has S waves with amplitudes large enough to be read (see Figs. 2 and 8). These facts precluded the use of only the S wave data to obtain an independent model of S velocity structure. Then we used S to P travel time ratios to calculate POISSON's ratios (σ) in the uppermost crust.

The S-times were picked with the help of low pass filtered records (Fig. 8). For each station and for each phase, S travel times Ts were divided by the corresponding P travel time Tp and these ratios Ts/Tp are plotted against distance from the shot in Fig. 9. Although scatter in the

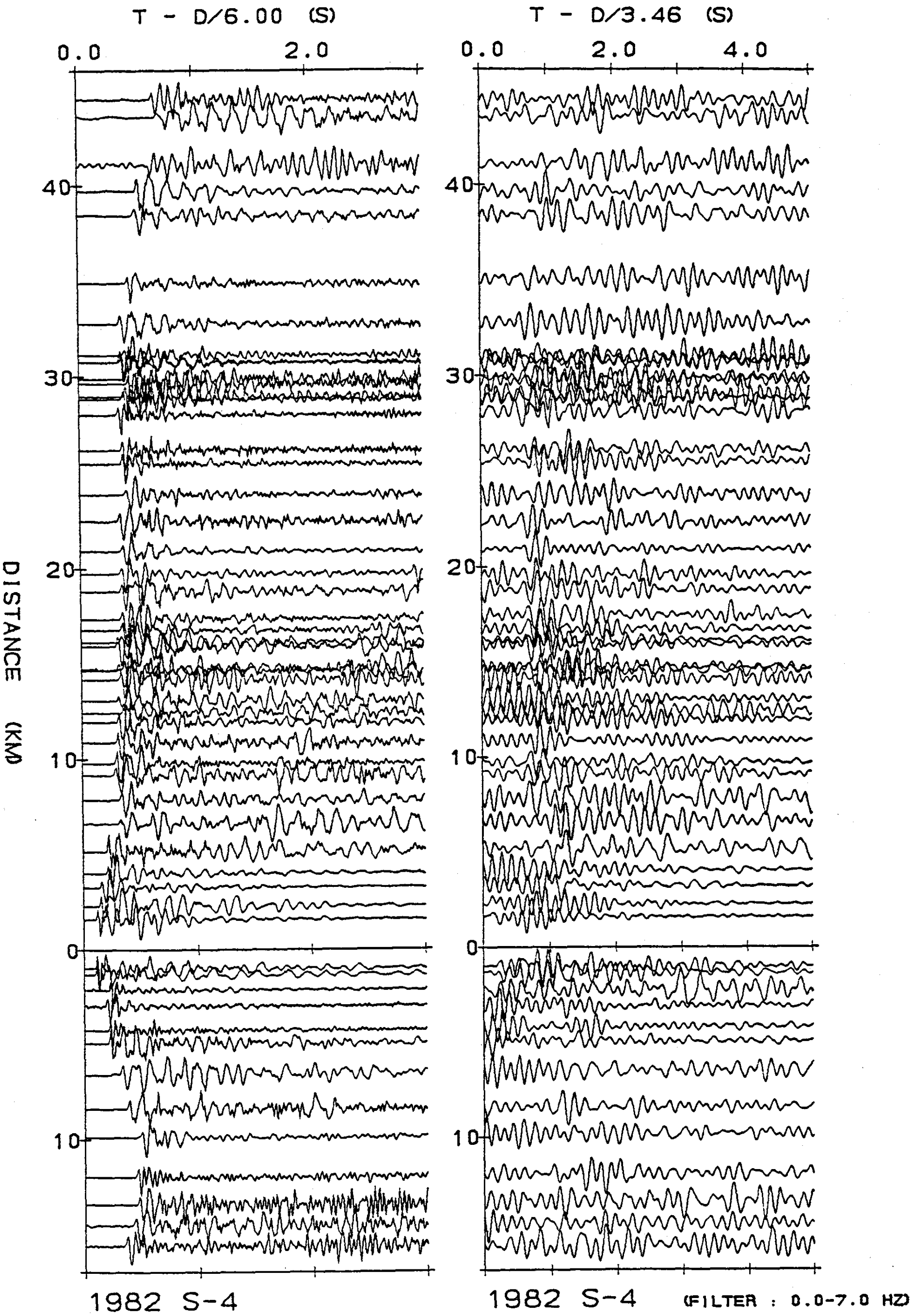

Fig. 8. P wave (a) and S wave (b) record sections for S-4. S wave, low pass filtered, record sections are plotted with a reduction velocity of 3.46 km/s and a time axis compressed by a factor of 1.73(=6/3.46) relative to the P wave section. This format allows easy comparison of S wave and P wave record sections: for POISSON's ratio of 0.25 throughout the crust, the S section overlay the P section.

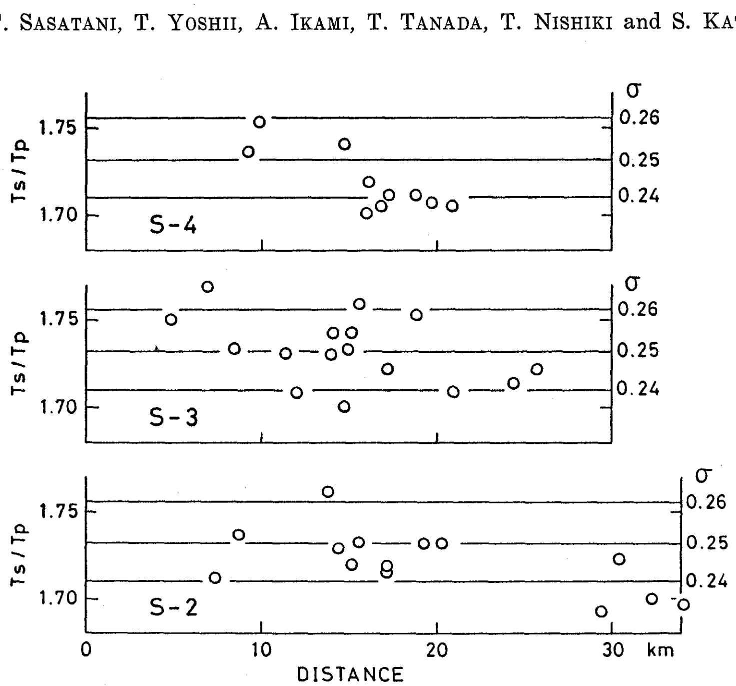

Fig. 9. *Ts/Tp* travel-time ratios for crustal refractions. The three horizontal lines are drawn at those values of *Ts/Tp* corresponding to $\sigma=0.26$, 0.25 and 0.24.

data is large due to the difficulty of reading shear waves and picking their onsets accurately, the ratios are in the range of 1.70 to 1.75 roughly independent of the shot points and distances. The average for all the data is $Ts/Tp=1.724$ which corresponds to $\sigma=0.246$. This value of POISSON's ratio is close to that generally observed in the uppermost crust, except for some sedimentary layers having a high ratio around 0.32 (*e.g.*, ASSUMPÇAO and BAMFORD, 1978; EL-ISA *et al.*, 1987; HOLBROOK *et al.*, 1988).

The later arrivals denoted by "R" in Fig. 2 can be seen more clearly on record sections of S-2 and S-5, as shown in Fig. 10. We mainly interpreted these data. The later arrivals are considered to be reflected phases from a deep interface, the Conrad discontinuity. The time differences between the first and the later arrivals for section S-5 are much smaller than those for section S-2. If we assume that these later arrivals are reflected phases from the same interface, this indicates that the interface inclines toward the north. We applied a simple ray-tracing technique to model the interface shape (IWASAKI, 1988). The upper crustal structure used in ray-tracing was constructed as follows: to a depth of 5 km we used the model obtained from the time-term method assuming the velocity

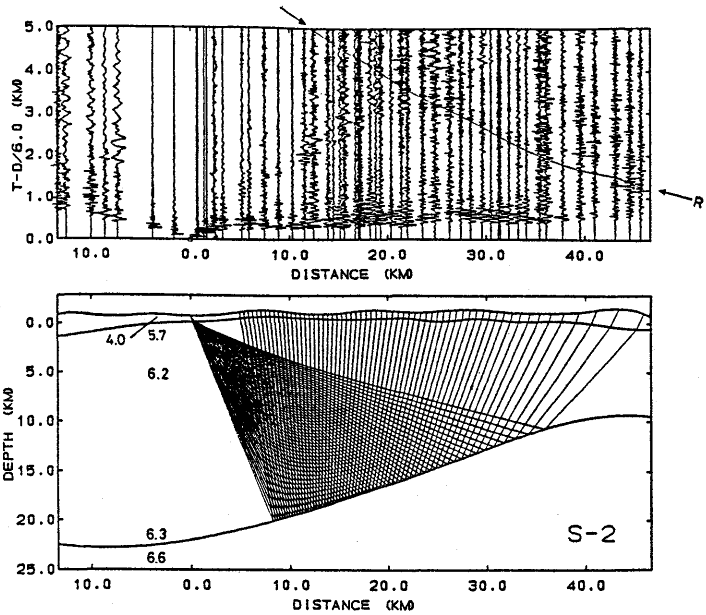

10(a)

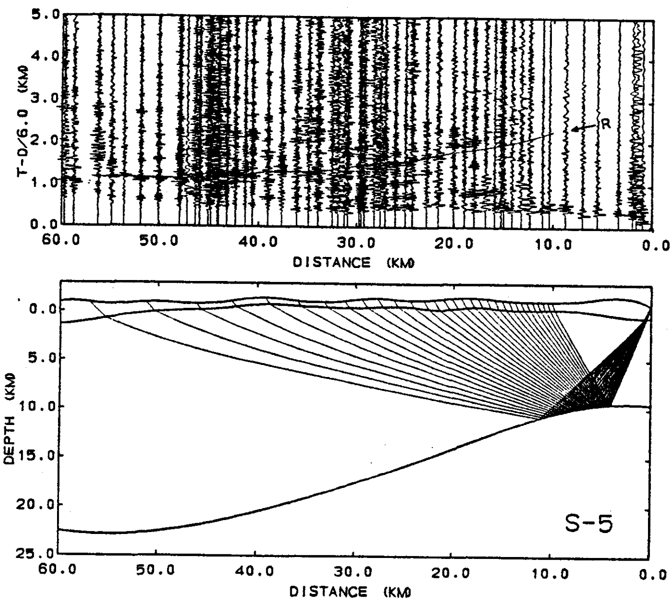

10(b)

Fig. 10. Upper: P wave record section with predicted travel times of reflected phases from the Conrad discontinuity. Reduction velocity is 6 km/s. Lower: Velocity structure model and ray diagram. Numbers indicate P wave velocity in km/s. (a) for shot S-2 and (b) for shot S-5.

gradient (Fig. 5); below that depth, since we have no information about velocity structure, we tentatively assumed a slight velocity gradient as shown in Fig. 10(a). The interface shape was iteratively improved by comparison of calculated travel times with observed ones. The final model is presented in Fig. 10 together with the ray diagram. The interface dip is about 20°. Of course, this model is not unique because there is no information about velocity structure beneath a depth of about 5 km, but the later arrivals "R" demonstrate the existence of the inclined Conrad discontinuity.

4. Conclusion

The upper crustal structure in the Miyota-Shikishima profile is simple compared with those beneath the Izu Peninsula and beneath the profile from southwestern Niigata Prefecture to western Nagano Prefecture (ASANO *et al.*, 1982; YOSHII *et al.*, 1985; IKAMI *et al.*, 1986). This structure, however, has a high velocity gradient in the uppermost crust; 4.0 km/s at the surface to 6.0 km/s at about 2.5 km depth. Based on the amplitude-distance study of the refraction phases we confirmed this conclusion. A few explosive sources generated strong S waves and S to P travel time ratios gave POISSON's ratio of around 0.246 in the uppermost crust. Generally S waves do not propagate very well through complex subsurface structures (ASSUMPÇAO and BAMFORD, 1978). Strong generation of S waves in this experiment may be caused by the simple structure and high velocity gradient. We observed the other later arrivals that were interpreted as reflected phases from a deep interface, the Conrad discontinuity. We modelled the interface shape by using a ray-tracing technique.

Acknowledgments

We wish to express our hearty gratitude to members of the Research Group for Explosion Seismology, especially those who participated in the experiment, for their advice and for placing the data at our disposal. We are grateful that the experiment for the study of the crustal structure could be carried out and was made possible by the Fund for Special Works of the Earthquake Research Institute, the University of Tokyo, as part of the Japanese Earthquake Prediction Project.

References

ASANO, S., T. YOSHII, S. KUBOTA, Y. SASAKI, H. OKADA, S. SUZUKI, T. MASUDA, H. MURAKAMI, N. NISHIDE and H. INATANI, 1982, Crustal structure in Izu Peninsula, Central Japan, as derived from explosion seismic observations. 1. Mishima-Shimoda Profile, *J. Phys. Earth*, **30**, 367-387.

ASSUMPÇAO, M. and D. BAMFORD, 1978, LISPB-V. Studies of crustal shear waves, *Geophys. J. R. astr. Soc.*, **54**, 61-73.

BANDA, E., N. DEICHMANN, L. W. BRAILE and J. ANSORGE, 1982, Amplitude study of the Pg phase, *J. Geophys.*, **51**, 153-164.

EL-ISA, Z., J. MECHIE and C. PRODEHL, 1987, Shear velocity structure of Jordan from explosion seismic data, *Geophys. J. R. astr. Soc.*, **90**, 265-281.

FUCHS, K. and G. MÜLLER, 1971, Computation of synthetic seismograms with the reflectivity method and comparison with observations, *Geophys. J. R. astr. Soc.*, **23**, 417-433.

HOLBROOK, W. E., D. GAJEWSKI, A. KRAMMER and C. PRODEHL, 1988, An interpretation of wide-angle compressional and shear wave data in southwest Germany: Poisson's ratio and petrological implications, *J. Geophys. Res.*, **93**, 12081-12106.

HOTTA, H., S. MURAUCHI, T. USAMI, E. SHIMA, Y. MOTOYA and T. ASANUMA, 1964, Crustal structure in Central Japan along longitudinal line 139°E as derived from explosion-seismic observations. Part 2. Crustal structure, *Bull. Earthq. Res. Inst., Univ. Tokyo*, **42**, 533-541.

IKAMI, A., T. YOSHII, S. KUBOTA, Y. SASAKI, A. HASEMI, T. MORIYA, H. MIYAMACHI, R. S. MATSU'URA and K. WADA, 1986, A seismic-refraction profile in and around Nagano Prefecture, Central Japan, *J. Phys. Earth*, **34**, 457-474.

IWASAKI, T., 1988, Ray-tracing program for study of velocity structure by ocean bottom seismographic profiling, *Zisin* II, **41**, 263-266, (in Japanese).

RESEARCH GROUP FOR ACTIVE FAULTS, 1980, Active faults in Japan, University of Tokyo Press, (in Japanese).

RESEARCH GROUP FOR EXPLOSION SEISMOLOGY, 1986, Explosion seismic observations in Nagano and Yamanashi Prefectures, Central Japan. Miyota-Shikishima Profile, *Bull. Earthq. Res. Inst., Univ. Tokyo*, **61**, 483-501, (in Japanese).

SASATANI, T., 1985, Seismic wave propagation in a stratified half-space, *J. Fac. Sci. Hokkaido Univ., Ser VII (Geophys.)*, **7**, 307-326.

YOSHII, T. and S. ASANO, 1972, Time-term analyses of explosion seismic data, *J. Phys. Earth*. **20**, 47-57.

YOSHII, T., S. ASANO, S. KUBOTA, Y. SASAKI, H. OKADA, T. MASUDA, T. MORIYA and H. MURAKAMI, 1985, Crustal structure in Izu Peninsula, Central Japan, as derived from explosion seismic Observations, 2. Ito-Matsuzaki Profile, *J. Phys. Earth*, **33**, 435-451.

日本中部下の上部地殻構造：御代田一敷島測線

北海道大学 笹谷 努
地震研究所 吉井敏尅
名古屋大学 伊神 煇
東海大学 棚田俊收*
地震研究所 西木 司**
北海道大学 加藤 進***

地震予知計画による4度目の爆破地震の実験が，1982年10月，日本中部の長野県から山梨県にかけての御代田一敷島測線上で行われた．60 km の測線上の5個所で爆破が行われ，約60点の臨時観測点で観測された．この実験の概要と，得られた記録や走時データなどの基礎的な資料については，すでに報告されている（爆破地震動研究グループ，1986）．ここでは，これらのデータの解析結果について報告する．

走時データから得られた上部地殻構造は，かなり単純で，横方向にほぼ均質である．しかし，それは大きい速度勾配を有している（地表での 4 km/s から約 2.5 km の深さでの 6 km までの P 波速度の増加）．走時データのみならず，初動の振幅一距離パタンもこの速度勾配モデルを支持する．本実験においては，2～3の爆破の際に明瞭なS波が観測された．S波とP波の走時比を使って上部地殻のポアソン比を求め，その平均値として 0.246 を得た．S波の他にもきわだった後続波が2～3の爆破の際に観測されている．これらをコンラッド面からの反射波とみなし，波線追跡法により，その形状として約20°の角度で北に向って傾く面を得た．

---

* 現在，温泉地学研究所，神奈川県
** 現在，石油資源開発(株)，東京
*** 現在，センチュリ リサーチ センター(株)，東京